2013

# Transferability of jarvis-type models developed and re-parameterized for maize to estimate stomatal resistance of soybean: analyses on model calibration, validation, performance, sensitivity, and elasticity

Denis Mutiibwa
*University of Nevada, Reno, Nevada*

Suat Irmak
*University of Nebraska-Lincoln*, suat.irmak@unl.edu

# Transferability of Jarvis-Type Models Developed and Re-Parameterized for Maize to Estimate Stomatal Resistance of Soybean: Analyses on Model Calibration, Validation, Performance, Sensitivity, and Elasticity

D. Mutiibwa, S. Irmak

**Abstract.** *In a previous study by the same authors, a new modified Jarvis model (NMJ-model) was developed, calibrated, and validated to estimate stomatal resistance ($r_s$) for maize canopy on an hourly time step. The NMJ-model's unique subfunctions, different from the original Jarvis model (J-model), include a photosynthetic photon flux density (PPFD)-$r_s$ response subfunction developed from field measurements and a new physical term, $A^{exp(1/LAI)}$, where A is the minimum stomatal resistance and LAI is the green leaf area index, to account for the influence of canopy development on $r_s$, especially during partial canopy stage in the early season and in late-season stage during leaf aging and senescence. This study evaluated the transferability of the J-model and NMJ-models that were re-parameterized and calibrated for maize canopy to estimate soybean $r_s$. Due to the differences in physiological and photosynthetic pathway differences between the two crops, the $r_s$ response to the same environmental variables, i.e., PPFD, vapor pressure deficit (VPD), and air temperature ($T_a$), were substantially different. Thus, this study demonstrated the inherent limitation in applying the Jarvis-type models that were calibrated for maize to soybean without re-calibration. Maize-calibrated models performed poorly in estimating soybean $r_s$, with the coefficient of determination ($r^2$) ranging from 0.30 to 0.38 and the root mean square difference (RMSD) between the estimated and measured $r_s$ ranging from 94.4 to 166 s $m^{-1}$. The J-model and NMJ-model were re-calibrated by parameter optimization method for soybean. The J-model calibrated well; however, the validation had poor performance results. The NMJ-model had a good calibration, resulting in a good $r^2$ (0.71) and a small RMSD (13.7 s $m^{-1}$). The NMJ-model validation produced superior results to the J-model, explaining more than 80% of the variation in the measured $r_s$ (RMSD = 38.4 s $m^{-1}$). These results show the robustness and practical accuracy of the NMJ-model in estimating $r_s$ over different canopies if well calibrated for a specific crop. In terms of sensitivity and elasticity analyses, among all parameters, $r_s$ estimates were most sensitive to uncertainties introduced in parameter $a_1$ of the PPFD subfunction due to its exponential impact on $r_s$ in the NMJ-model. Therefore, for accurate estimates of $r_s$, uncertainties in parameter $a_1$ should not exceed the range of -2% and 2% so that the error in estimated $r_s$ is kept between -3.5% and 3.6%. The study observed that the relative change in $r_s$ due to uncertainties in parameters $a_2$ and $a_3$ of the VPD subfunction was a linear function and less sensitive than the PPFD subfunction. The sensitivity of $r_s$ to uncertainties in temperature subfunction parameters ($a_4$ and $a_5$) was higher than that of VPD subfunction parameters, but less than that of PPFD subfunction parameters. The uncertainty in parameters $a_4$ and $a_5$ should range within -10% and 10%, and the calibration of these parameters should be determined with greater precision as compared with the VPD subfunction parameters. The study confirmed that the addition of the $r_{s\_min}$ and the $A^{exp(1/LAI)}$ terms, which were not accounted for in the original J-model, improved the model accuracy for estimating soybean $r_s$.*

***Keywords.*** *Elasticity analyses, Jarvis model, Maize, Optimization, Sensitivity analysis, Soybean, Stomatal resistance.*

Stomatal resistance ($r_s$) is an important and intricate phenomenon that is essential to understanding plant-soil-water-atmosphere relationships and to evaluating plant responses to various environmental variables. It is one of the drivers of photosynthesis and transpiration processes, which ultimately determine crop water productivity (also known as crop water use efficiency) and many other plant physiological functions. The phenomenon crucially regulates the biophysical link between the water source (soil moisture) and the atmospheric evaporative demand. The $r_s$ is subject to independent and interactional influence of plant physiology, soil physical and chemical properties and moisture content, and atmospheric conditions. With tre-

Submitted for review in May 2012 as manuscript number SW 9769; approved for publication by the Soil & Water Division of ASABE in March 2013.

The mention of trade names or commercial products is for the information of the reader and does not constitute an endorsement or recommendation for use by the University of Nebraska-Lincoln or the authors.

The authors are **Denis Mutiibwa, ASABE Member,** Post-Doctoral Research Associate, Department of Geography, University of Nevada, Reno, Nevada; and **Suat Irmak, ASABE Member,** Professor, Department of Biological Systems Engineering, University of Nebraska-Lincoln, Lincoln, Nebraska. **Corresponding author:** Suat Irmak, 239 L. W. Chase Hall, University of Nebraska-Lincoln, Lincoln, NE 68583, phone: 402-472-4865; e-mail: sirmak2@unl.edu.

  ISSN 2151-0032 

mendous labor and cost, continuous and viable measurements of $r_s$ can be made using either steady-state or dynamic diffusion porometry instrumentation. Porometers measure $r_s$ by predicting the change in water vapor diffusion rate from a porous surface of the leaf in an enclosed chamber. The measurements are referenced to a pre-calibration fit of a standard porous surface of know diffusion resistances. The $r_s$ and stomatal aperture and behavior can also be measured and monitored using observations under a microscope, using cobalt-chloride paper, the leaf-chamber (cuvette) transpiration method, and mass-flow porometry methods (Kirkham, 2005, pp. 392-393).

For years, strenuous research has advanced efforts to model $r_s$ from soil moisture, carbon dioxide concentrations, and climatic variables. However, the physiological knowledge about stomatal functioning may not be adequate to provide a mechanistic model linking stomatal resistance to all driving variables. The alternative approach is to estimate $r_s$ phenomenologically from environmental variables. Jarvis (1976) developed a descriptive and multiplicative model to estimate stomatal resistance as a function of environmental variables, soil moisture, and plant water status. The model predicted the response of stomata to environmental variables operating as resistance stress functions without synergy. Jarvis (1976) described the model (J-model) as a useful interim way of using field measurements to describe very complex and changing properties of the stomata. Since its development, the model has been extended, recalibrated, and/or re-parameterized into various Jarvis-type models for different vegetation surfaces and environmental conditions (Farquhar, 1978; Farquhar et al., 1980; Lohammar et al., 1980; Kauffman, 1982; Jarvis and McNaughton, 1986; Ball et al., 1987; Noilhan and Planton, 1989; Massman and Kaufmann, 1991; Pleim and Xiu, 1995; Viterbo and Beljaars, 1995; Niyogi and Raman, 1997; Green and McNaughton, 1997; Thomas et al., 1999; Irmak and Mutiibwa, 2009, 2010).

In the Irmak and Mutiibwa (2009) study, a new modified Jarvis model (NMJ-model) was presented along with the original Jarvis (1976) and Green and McNaughton (1997) models, and Irmak and Mutiibwa (2009) calibrated/re-parameterized and validated the NMJ-model against porometer-measured $r_s$ data through extensive field measurements for a non-stressed maize canopy. The new re-parameterized NMJ-model was developed with a new physical term: $A^{\exp(1/\mathrm{LAI})}$, where $A$ is the minimum leaf stomatal resistance (s m$^{-1}$), and LAI is the leaf area index (unitless) to account for the influence of canopy development on $r_s$, especially during the partial canopy cover stage. The vital $r_s$ response to light was modeled based on the photosynthetic photon flux density (PPFD) vs. $r_s$ response curves that were measured in the field. The NMJ-model demonstrated improved performance over the original Jarvis (1976) model (J-model) in estimating hourly $r_s$, especially during the partial canopy cover stage. The calibration and the new physical term accounting for the variation in LAI improved the $r_s$ modeling performance. Irmak and Mutiibwa (2009) demonstrated that on a seasonal average basis, the J-model and the NMJ-model had similar performance in estimating $r_s$, with a coefficient of determination ($r^2$) of 0.74 and a root mean square difference (RMSD) between the modeled and measured $r_s$ of 48.8 s m$^{-1}$ for the J-model, and $r^2$ = 0.74 and RMSD = 50.1 s m$^{-1}$ for the NMJ-model, for a non-stressed, subsurface drip-irrigated maize canopy. The inclusion of the variation in the LAI and $r_{s\_min}$ term [$r_{s_min}$exp(-LAI)] during the growing season in the NMJ-model improved the $r_s$ estimation, especially in the higher $r_s$ range ($r_s$ > 250 s m$^{-1}$), as compared to the J-model. When the period of partial canopy cover was considered separately (LAI range from 1.20 to approximately 2.5), the addition of the LAI term in the NMJ-model resulted in 8% improvement in $r^2$ and 10% improvement in RMSD relative to the J-model ($r^2$ = 0.64, RMSD = 35.5 s m$^{-1}$ for the NMJ-model, and $r^2$ = 0.59, RMSD = 39.0 s m$^{-1}$ for the J-model). The enhanced performance of the NMJ-model was attributed to the calibration of the model to a specific crop and environmental conditions. In another study by Noilhan and Planton (1989), the J-model was extended and improved through environmental modulation of minimum stomatal resistance and by the integration of the inverse LAI effect on $r_s$. Although Jarvis (1976) did not include variable LAI in his original $r_s$ model, the variability of LAI is known to control the amount of light scattered and absorbed by the plant canopy, impacting stomatal functions and responses. Finnigan and Raupach (1987) linked LAI, theoretically, to the vegetation's diffusive source/sink capacity, which regulates the mass and energy exchange rate of the plant canopy via stomatal regulation.

The Jarvis-type models have proved to be practical in modeling $r_s$; however, their empirical development is, in principal, a limitation in their transferability to estimate $r_s$ for different crops. Since different plant species (e.g., maize vs. soybean) have different stomatal response to the same environmental variable, a model that was developed for maize canopy may not accurately represent stomatal behavior of soybean canopy. Because maize and soybean are the dominant agronomic crops produced in Nebraska and many other Midwestern U.S. states, and in many other countries, there is a need to test the maize $r_s$ models' performances for estimating soybean $r_s$ and potentially develop new models or re-calibrate/re-parameterize the maize $r_s$ model for soybean canopy. In the research conducted by Irmak and Mutiibwa (2009), the NMJ-model was developed for maize canopy under south central Nebraska environmental and climatic conditions and management practices. The three main objectives of this research were to: (1) evaluate the transferability of the two $r_s$ models, the J-model (Jarvis, 1976) and the NMJ-model (Irmak and Mutiibwa, 2009), that were calibrated and re-parameterized for non-stressed maize canopy to estimate $r_s$ for soybean canopy; (2) recalibrate the models to estimate $r_s$ for soybean, using extensive datasets measured through an independent field campaign for soybean, by applying the same approach presented by Irmak and Mutiibwa (2009); and (3) investigate the sensitivity of $r_s$ to the NMJ-model coefficients in the subfunctions of environmental variables in the model. The models were recalibrated and validated using data from extensive field measurements of $r_s$, climatic variables, plant physiology parameters, and soil water status in the 2007 soybean growing season in south central Nebraska.

## MATERIALS AND METHODS

### STUDY SITE

The field measurements for this study were conducted in 2007 at the University of Nebraska-Lincoln, South Central Agricultural Laboratory (SCAL) near Clay Center, Nebraska. The site is located in Clay County in the south central part of the state at 40° 34′ N and 98° 8′ W at an elevation of 552 m above mean sea level (Irmak, 2010). The soil at the site is a Hastings silt loam (fine, montmorillonitic, mesic Udic Argiustoll), with 0.5% slope, which is a well-drained soil on uplands, with field capacity of 0.34 $m^3$ $m^{-3}$, permanent wilting point of 0.14 $m^3$ $m^{-3}$, and saturation point of 0.53 $m^3$ $m^{-3}$. The particle size distribution is 15% sand, 65% silt, and 20% clay, with 2.5% organic matter content in the topsoil (Irmak, 2010). The experimental field is 13 ha in size and irrigated with a subsurface drip irrigation system. The drip lines were installed at about 0.40 m below the soil surface with 0.45 m emitter spacing on the drip lines and 1 LT $h^{-1}$ flow rate with pressure-compensating drip emitters (Netafim-USA, Fresno, Cal.). The field was irrigated two or three times per week to meet plant water requirement. The soil water content was measured using a neutron probe soil moisture meter (model 4302, Troxler Electronics Laboratories, Inc., N.C.) at 0.30, 0.60, 0.90, and 1.20 m soil depths twice a week throughout the season. For each irrigation application, the soil water deficit was replenished to approximately 90% of the field capacity in the top 0.90 m soil profile to maintain non-stressed plant conditions and to reserve storage in the soil profile for potential rainfall. The effective rooting depth for soybean in the experimental region is 0.90 m. The total available water holding capacity of the top 0.90 m soil profile is approximately 175 mm. The maximum allowable depletion was set to approx.-imately 40% to 45% of the total available water. A total of seven irrigations were applied during the 2007 growing season [July 23 (9 mm), July 26 (13 mm), August 7 (17 mm), August 10 (13 mm), August 13 (26 mm), August 16 (21 mm), and August 20 (11 mm)] with a seasonal total of 110 mm. The total rainfall from emergence until physiological maturity (May 26 to September 30) measured in the experimental field was 354 mm. Plants were maintained with regular pest and disease control practices when needed (Irmak, 2010). The soybean [*Glycine max* (L.) Merr.] crop was planted on May 21 with a planting density of approximately 188,000 plants $ha^{-1}$. The planting row spacing was 0.762 m with a west-east planting direction. Plants emerged on May 26, reached flowering stage around July 14-15, reached pod formation stage (R3) around July 20, reached complete canopy closure around August 2 (73 days after planting), fully matured on September 30, and were harvested on October 24, 2007 (Irmak, 2010).

### MICROMETEOROLOGY MEASUREMENTS

Measurements of surface energy fluxes (including latent heat flux ($ET_a$), sensible heat flux, soil heat flux, and net radiation) and other climatic variables (air temperature, relative humidity, wind speed and direction, and precipitation) were made using a Bowen ratio energy balance system (BREBS) (Radiation and Energy Balance Systems (REBS), Inc., Bellevue, Wash.), which was stationed in the middle of the experimental field (Irmak, 2010). The site and the BREBS are part of the Nebraska Water and Energy Flux Measurement, Modeling and Research Network (NEBFLUX; Irmak, 2010), which is a network of 11 flux towers that are installed and operated on an hourly basis in various parts of Nebraska on vegetation surfaces ranging from irrigated and rainfed croplands, including maize (*Zea mays* L.), soybean [*Glycine max* (L.) Merr.], and winter wheat (*Triticum aestivum* L.) under different tillage and irrigation practices; irrigated and natural grasslands, including mixture of tall fescue (*Festuca arundinacea*), Kentucky bluegrass (*Poa pratensis*), smooth bromegrass (*Bromus inermis*), creeping foxtail (*Alopecurus arundinacea*), and buffalograss (*Bouteloua dactyloides* Nutt.); irrigated alfalfa (*Medicago sativa* L.); and rainfed switchgrass (*Panicum virgatum*) to riparian systems with invasive plant species [common reed (*Phragmites australis*), peach-leaf willow (*Willow salix*), and cottonwood (*Populus deltoides* var. *occidentalis*), etc.). The NEBFLUX towers measure all surface energy flux variables, meteorological variables, plant physiological parameters, soil water content (every 0.30 m up to 1.80 m on an hourly basis), soil characteristics, and agronomical components, including biomass production and/or yield, for a significant number of different vegetation surfaces. For this study, net radiation ($R_n$) was measured using a REBS model Q*7.1 net radiometer. Incoming and outgoing shortwave and longwave radiation were measured simul-taneously using a REBS model THRDS7.1 double-sided total hemispherical radiometer that is sensitive to wave-lengths from 0.25 to 60 μm (Irmak, 2010). Air temperature ($T_a$) and relative humidity (RH) gradients were measured using two platinum resistance thermometers and monolithic capacitive humidity sensors (REBS models THP04015 and THP04016, respectively) with resolutions of 0.0055°C for temperature and 0.033% for relative humidity. The measured temperature and relative humidity gradients were used to calculate vapor pressure deficit (VPD). Preci-pitation was recorded using a sensor (model TR-525, Texas Electronics, Inc., Dallas, Tex.). Wind speed and direction at 3 m height were monitored using a cup anemometer (model 034B, Met One Instruments, Grant Pass, Ore.). The anemometer had a wind speed range of 0 to 44.7 m $s^{-1}$ and threshold wind velocity of 0.28 m $s^{-1}$. The BREBS used an automatic exchange mechanism that physically exchanged the temperature and humidity sensors every 15 min at two heights above the canopy. All variables were sampled every 60 s, averaged, and recorded on an hourly basis using a CR10X datalogger and AM416 relay multiplexer (Camp-bell Scientific, Inc., Logan, Utah) (Irmak, 2010). Extensive maintenance procedures that were described by Irmak (2010) were followed weekly to ensure continuous and good quality data collection throughout the year. Additional detailed description of the BREBS setup and instrumentation are provided by Irmak (2010).

### STOMATAL RESISTANCE, PLANT GREEN LAI, AND PLANT HEIGHT MEASUREMENTS

The plant variables measured included $r_s$, green LAI, and plant height ($h$). A dynamic diffusion porometer (model AP4, Delta-T Devices, Ltd., Cambridge, U.K.) equipped with an unfiltered GaAsP photodiode light sensor with a spectral response similar to photosynthetically active radiation response (Irmak and Mutiibwa, 2009; Mutiibwa and Irmak, 2011) was used to measure $r_s$ on randomly selected green and healthy soybean leaves. Before taking readings, the porometer was calibrated based on the manufacturer's recommendations. The unit was recalibrated every time RH changed by ±10% from the previously set value and whenever air temperature changed by ±4°C from the temperature at the time of previous calibration. The porometer head unit contained fast-response sensors to measure cup and leaf temperatures, allowing automatic temperature compensation to be applied when measuring $r_s$. The AP4 porometer has a resolution of 0.5 mol $m^{-2}$ $s^{-1}$ with an $r_s$ measurement speed of less than 5 s. For each $r_s$ measurement cycle, the following variables were recorded simultaneously: $r_s$ (s $m^{-1}$), PPFD (mol $m^{-2}$ $s^{-1}$), chamber (cup) temperature ($T_c$, °C), and leaf-chamber temperature difference ($T_L - T_c$, °C). On a given field measurement day, on average, three readings from each leaf, six leaves from each plant, and fifteen to thirty plants were sampled for $r_s$ measurements and averaged per hour. Each reading corresponded to one complete diffusion cycle in which the sensor and leaf reached equilibrium with the RH in the chamber. This study uses the $r_s$ data, PPFD vs. $r_s$ response curves, and other supporting field data that were measured by Mutiibwa and Irmak (2011). The reader is referred to Mutiibwa and Irmak (2011) for more detailed description of the field measurement. LAI was measured using a plant canopy analyzer (model LAI-2000, Li-Cor Biosciences, Lincoln, Neb.) once a week during the growing season. On average, a total of 60 LAI measurements were taken across the field on each field measurement day and averaged for that day. LAI measurements were started at 32 days after planting (DAP) (June 22) when LAI was approximately 1.10. On the same days of LAI field measurements, plant height ($h$) measurements were taken by measuring soybean plants from the soil surface to the tip of the tallest leaf for 14 to 17 randomly selected plants, and the values were averaged for that week.

### JARVIS MODEL (J-MODEL)

The J-model (Jarvis, 1976) estimates $r_s$ as a function of multiplicative subfunctions of environmental and plant physiological variables without synergistic interaction. The subfunction variables include PPFD (µmol $m^{-2}$ $s^{-1}$), VPD (kPa), air temperature ($T_a$), soil water content ($W$, % vol), and maximum stomatal conductance ($b_1$, m $s^{-1}$). The model is expressed as:

$$r_s = F_1^{-1} F_2^{-1} F_3^{-1} F_4^{-1} \tag{1}$$

$$F_1 = \frac{b_1 b_2 \left(\text{PPFD} - q\right)}{\left[b_1 + b_2 \left(\text{PPFD} - q\right)\right]} \tag{2}$$

$$F_2 = \left[1 - b_3 \left(\text{VPD}\right)\right]^{b_4} \tag{3}$$

$$F_3 = 1 - b_5 \left(298 - T_a\right)^2 \tag{4}$$

$$F_4 = \begin{cases} 1, & \text{if } w_2 > w_{cr} \\ \dfrac{w_2 - w_{wilt}}{w_{cr} - w_{wilt}}, & \text{if } w_{wilt} \leq w_2 \geq w_{cr} \\ 0, & \text{if } w_2 > w_{cr} \end{cases} \tag{5}$$

where $F$ is the subfunction that describes the stomatal response to a particular variable such that $0 < F < 1$, although not always. $F_1$ is the subfunction that describes the $r_s$ response to PPFD, $q$ (s $m^{-1}$) is the asymptotic value of stomatal conductance ($g$, m $s^{-1}$) ($1/r_s$) at infinite PPFD. Based on the asymptote from the PPFD-$r_s$ response curve of soybean presented by Mutiibwa and Irmak (2011), $q$ was set to 0.0289 s $m^{-1}$. The parameter $b_1$ is the maximum $g$ at full sunlight and is calculated from the relationship $q = b_0/(b_1)^2$, where $b_0$ is the nocturnal (night time) $g$. Parameter $b_2$ (µmol $m^{-2}$ $s^{-1}$) is the slope of the PPFD vs. $r_s$ response curve at PPFD = 0. $F_2$ is the subfunction that describes the $r_s$ response to VPD. The parameter $b_3$ ($Mg^{-1}$ $s^3$) in equation 3 represents the slope of the relationship between $r_s$ and VPD. $F_3$ is the subfunction that describes the $r_s$ response to $T_a$ (in K). The subfunction $F_4$ accounts for the effect of crop water stress on $r_s$. It varies between 0.0 and 1.0 when soil water content ($w_2$, % vol) varies between permanent wilting point ($w_{wilt}$) and a critical value ($w_{cr}$) at $0.75w_{sat}$ (Thompson et al., 1981), where $w_{sat}$ represents the volumetric soil water content (% vol) at saturation. The term $w_2$ represents the deep soil profile moisture (volumetric water content at 1 m below the soil surface). In this study, the soil moisture at the effective plant root zone depth was maintained at optimum level (i.e., $w_2 > w_{cr}$); therefore, $F_4$ was taken as 1.0.

### NEW MODIFIED JARVIS (NMJ) MODEL

The NMJ-model that was developed for maize canopy was presented by Irmak and Mutiibwa (2009). The important features of the new model included the PPFD-$r_s$ response function for the crop canopy, which was measured and constructed in the field to account for the effect of different ranges of canopy light distribution on $r_s$. The PPFD vs. $r_s$ response function replaced the $F_1$ subfunction in the J-model (eq. 1). The NMJ-model has a new term extension that integrates the effect of LAI variation on $r_s$ during the growing season. The original J-model did not account for the LAI effect on $r_s$. However, LAI has an important role in driving stomatal behavior. To account for the effect of seasonal variation of LAI on $r_s$, an extension term of $r_{s\_min}$ was raised to the inverse exponential function of LAI and incorporated into the NMJ-model, as shown in equation 6:

$$r_s = a_0 \left(\text{PPFD}\right)^{a_1} \times \left(1 - a_2 \text{VPD}\right)^{a_3} \times \left[1 - a_4 \left(298 - T_a\right)\right]^{a_5} + r_{s\_min}{}^{(1/\text{expLAI})} \quad (6)$$

where PPFD (μmol m$^{-2}$ s$^{-1}$) is measured or estimated at the leaf level, VPD is in kPa, and $T_a$ is in K. The parameter $a_0$ is the slope of the PPFD vs. $r_s$ response subfunction (measured as 3010 s m$^{-1}$ by Mutiibwa and Irmak, 2011), $a_1$ is the exponent of the measured PPFD-$r_s$ response subfunction, parameters $a_2$ and $a_3$ represent the coefficients in the VPD subfunction, and parameters $a_4$ and $a_5$ represent the coefficients in the $T_a$ subfunction. The term $r_{s\_min}$ (s m$^{-1}$) represents the lowest (minimum) measured $r_s$ during the growing season. Based on our extensive field measurements, $r_{s\_min}$ for soybean canopy is 22.4 s m$^{-1}$.

### J-Model and NMJ-Model Calibration and Optimization

In the Irmak and Mutiibwa (2009) study, the J-model and NMJ-model were calibrated for maize for the 2006 growing season. Therefore, we first evaluated the transferability of the maize-calibrated models to estimate $r_s$ for soybean in the 2007 growing season. The performances of the models were evaluated using RMSD, r$^2$, and modeling efficiency (unitless), which is expressed as:

$$\text{EF} = 1 - \frac{\sum \left(O_i - P_i\right)^2}{\sum \left(O_i - \overline{O}\right)^2} \quad (7)$$

where $O_i$ and $P_i$ are the observed and predicted $r_s$, respectively, and $\overline{O}$ is the mean of observed data. The models were re-calibrated and re-parameterized for soybean by applying the parameter optimization procedure and then validated using porometer-measured soybean $r_s$. The days for the soybean stomatal resistance measurements were randomly and evenly divided to create two datasets: one for calibration, and one for validation. The dates and meteorological conditions on the days when the $r_s$ measurements were made for model calibration and validation are presented in table 1. Using the Solver tool in Microsoft Excel 2010, the parameters of the models were optimized for the best-fit model on measured $r_s$ by minimizing RMSD and maximizing r$^2$. The procedure of optimization involves searching the parameter space for a parameter value that is optimal with respect to the specified objective conditions, such as minimizing RMSD and maximizing r$^2$. The RMSD evaluates the accuracy of the optimized model by measuring the deviation of the model estimates from the measured $r_s$. During the optimization process, a constraint was added by holding the regression slope of the estimates on measured $r_s$ between 0.90 and 1. A constraint is a logical condition that an optimized model must satisfy. The calibrated model performance was evaluated using EF (eq. 7), which assesses the fraction of the variance of the measured values that is explained by the model. The EF ranges between one and negative infinity, and values close to unity are an indication of good performance of the model. The validation of the models was implemented by using the models to estimate soybean $r_s$ and compare the model-estimated results to measured soybean $r_s$ using the validation dataset. The validation performance statistics are presented in table 3 for the model calibration and validation.

### Sensitivity and Elasticity Analysis

The technique of parameter optimization is implemented by searching, under specified conditions, the parameter space to find the optimal parameters for the best fit in a model. Therefore, by applying sensitivity and elasticity analysis on the NMJ-model parameters, the study analyzes the potential variations and errors in the estimated $r_s$ originating from the potential parameter uncertainties over the parameter space. The analysis objectives are to determine the important parameters, which cause the most significant variations in estimated $r_s$; determine the type of sensitivity and elasticity functions; identify threshold values where the optimal strategy changes; and determine the relative variation (uncertainty percentages) in each parameter for practically accurate $r_s$ estimates.

For most sensitivity analysis studies, the focus usually is to evaluate the relative error induced in the model output due to potential uncertainties and errors and the magnitude of changes in the input variables. In the NMJ-model sensitivity and elasticity analysis, the relative error introduced in estimated $r_s$ by the input parameter's potential relative variation over the parameter space during the optimization process was evaluated. By holding all variables and parameters constant, the sensitivity of $r_s$ to the variation in a given parameter was investigated by systematically varying the calibrated value of the investigated parameter within the conceivable range. This technique of sensitivity analysis is referred to as one-at-a-time sensitivity analysis (Hamby, 1994). Each parameter

**Table 1. Daily average meteorological variables measured during the 2007 growing season when stomatal resistance ($r_s$) measurements were made. Variables include incoming shortwave radiation ($R_s$), net radiation ($R_n$), maximum and minimum air temperature ($T_{a\_max}$ and $T_{a\_min}$), wind speed at 3 m ($u_3$), maximum and minimum relative humidity (RH$_{max}$ and RH$_{min}$), vapor pressure deficit (VPD), and rainfall.**

| | Date (2007) | $R_s$ (W m$^{-2}$) | $R_n$ (W m$^{-2}$) | $T_{a\_max}$ (°C) | $T_{a\_min}$ (°C) | RH$_{max}$ (%) | RH$_{min}$ (%) | $u_3$ (m s$^{-1}$) | VPD (kPa) | Rainfall (mm) |
|---|---|---|---|---|---|---|---|---|---|---|
| Calibration | 16 July | 300 | 196 | 31.5 | 16.2 | 99.1 | 55.7 | 2.4 | 2.3 | 0 |
| | 20 July | 223 | 143 | 28.0 | 19.4 | 95.2 | 75.6 | 3.4 | 2.5 | 4.6 |
| | 26 July | 293 | 192 | 32.8 | 19.0 | 95.0 | 48.0 | 3.0 | 2.3 | 0 |
| | 31 Aug. | 248 | 157 | 27.0 | 13.4 | 100.0 | 63.2 | 2.3 | 2.0 | 0 |
| Validation | 24 July | 294 | 193 | 30.4 | 20.8 | 100.0 | 62.3 | 2.3 | 2.7 | 0 |
| | 9 Aug. | 290 | 195 | 32.5 | 19.6 | 100.0 | 60.4 | 1.9 | 2.9 | 0.25 |
| | 14 Aug. | 280 | 181 | 35.2 | 20.4 | 82.2 | 39.9 | 2.2 | 2.2 | 0 |
| | 12 Sept. | 237 | 138 | 26.0 | 08.4 | 98.0 | 41.8 | 3.7 | 1.3 | 0 |

Meteorological Variable spans the columns from $R_s$ to Rainfall.

was deviated from the baseline value (optimized or calibrated value) by -99%, -75%, -50%, -25%, -10%, -5%, -2%, -1%, 1%, 2%, 5%, 10%, 25%, 50%, 75%, and 100%. The sensitivity analysis was carried out on field measurement days when data were collected for calibration, as shown in table 1. For each parameter value's deviation from the baseline, the $r_s$ relative error (%) was averaged over the calibration days. To determine the important parameters that cause the most variations in estimated $r_s$, the elasticities, which are measures of the percent change in a dependent variable ($r_s$) divided by the percent change in an independent variable (parameter), were calculated using equation 8:

$$E = \frac{\%\Delta Y}{\%\Delta X} \tag{8}$$

Essentially, the elasticities ($E$) of parameters are the first derivatives of the sensitivity function. For linear sensitivity functions, the elasticities are constant values; however, for non-linear sensitivity functions, the elasticities are first-derivative functions of the sensitivity functions. This analysis identifies parameter spaces where the response of $r_s$ is elastic or inelastic. An elastic response is one in which $r_s$ responds highly to small changes in the parameter, whereas an inelastic response is one in which $r_s$ does not respond much to the changes in the parameter.

# Results and Discussion

## Weather Conditions During Research Period

A summary of the daily average meteorological conditions for the 2007 growing season and their comparisons relative to the long-term (32-year) averages are presented in table 2, and daily rainfall events and seasonal cumulative values are presented in figure 1. During the growing season, the total rainfall from May through end of September (473 mm) was very close to the long-term growing season average value (461 mm). The largest rainfall event occurred on August 22 as 80 mm. Another large rainfall was recorded on July 9 as 56 mm. Although July and August were wetter than the long-term average, the rainfall amount from after July 9 until August 22 was not enough to meet crop water requirement. The seasonal average wind speed was 13% greater than the long-term average, with the highest monthly average wind speed occurring in May (5.0 m s$^{-1}$). $T_{a\_max}$ was very close to

**Table 2. Daily average meteorological variables measured from May to October 2007 and long-term averages at Clay Center, Nebraska. Variables include wind speed at 3 m ($u_3$), maximum and minimum air temperature ($T_{a\_max}$ and $T_{a\_min}$), relative humidity (RH), incoming shortwave radiation ($R_s$), and total rainfall.**

| Period | Meteorological Variable | May | June | July | August | September | October |
|---|---|---|---|---|---|---|---|
| 2007 | $u_3$ (m s$^{-1}$) | 5.0 | 3.9 | 2.8 | 3.0 | 3.6 | 3.8 |
| | $T_{a\ max}$ (°C) | 23.5 | 27.1 | 29.3 | 29.5 | 25.1 | 19.6 |
| | $T_{a\ min}$ (°C) | 12.5 | 15.4 | 18.5 | 19.0 | 11.5 | 6.7 |
| | RH (%) | 71.6 | 72.9 | 77.8 | 81.3 | 73.3 | 71.5 |
| | $R_s$ (MJ m$^{-2}$ d$^{-1}$) | 19.9 | 22.9 | 22.0 | 18.3 | 16.4 | 11.8 |
| | Rainfall (mm) | 130 | 53 | 106 | 117 | 67 | 149 |
| Long-term (32-year) average | $u_3$ (m s$^{-1}$) | 4.0 | 3.5 | 2.9 | 2.6 | 3.1 | 3.3 |
| | $T_{a\ max}$ (°C) | 22.5 | 28.1 | 30.3 | 29.2 | 25.3 | 18.3 |
| | $T_{a\ min}$ (°C) | 9.3 | 14.6 | 17.3 | 16.3 | 10.7 | 3.6 |
| | RH (%) | 71.3 | 70.2 | 73.2 | 74.5 | 68.8 | 67.2 |
| | $R_s$ (MJ m$^{-2}$ d$^{-1}$) | 19.4 | 22.4 | 22.4 | 19.7 | 15.9 | 11.3 |
| | Rainfall (mm) | 112 | 110 | 93 | 83 | 63 | 45 |

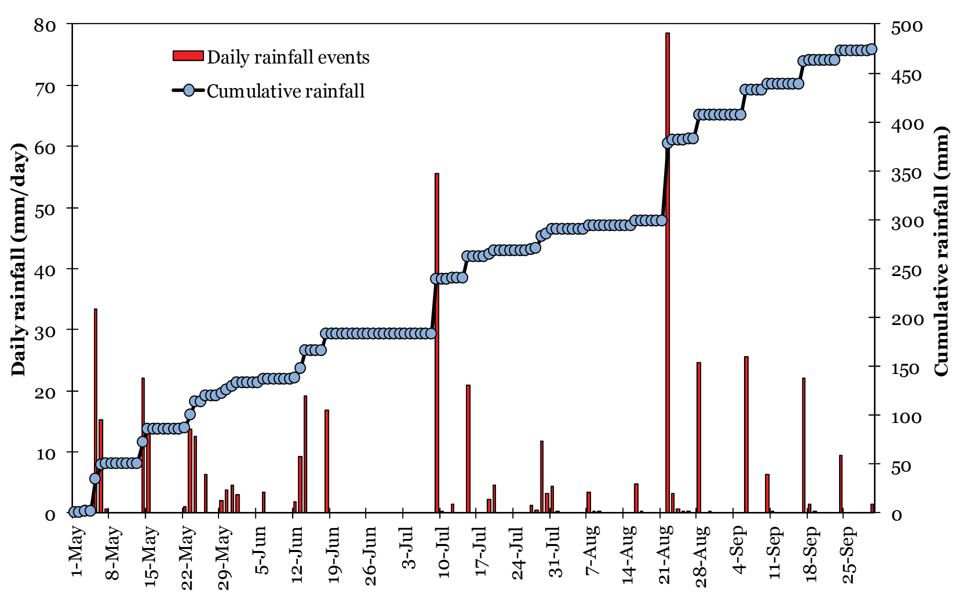


**Figure 1. Daily rainfall events and cumulative seasonal rainfall measured in the experimental field from May 1 through October 31, 2007.**

the average, but on average $T_{a\_min}$ was approximately 16% higher than normal. The seasonal average relative humidity was about 5% more than long-term average.

### Seasonal Trend of Measured Soybean Stomatal Resistance

Figure 2 presents the seasonal trend in measured hourly soybean $r_s$ and daily soybean LAI. For each $r_s$ measurement day, there are several hours of data points showing the daily range of $r_s$. For example, on July 20, the measured $r_s$ ranged from 108 s m$^{-1}$ at 9:00 a.m. to the lowest value of 24 s m$^{-1}$ at solar noon at 3:00 p.m., with a large diurnal range of 84 s m$^{-1}$. There was an opposite trend between LAI and $r_s$. Although partly obscured by the hourly fluctuations on measurement days, the $r_s$ trend depicts the theoretical parabolic variation of $r_s$ that was also observed by Monteith (1965), Monteith et al. (1965), and Irmak and Mutiibwa (2009). The $r_s$ exhibited a decreasing trend from early season toward mid-season and remained relatively constant, with later increases toward the end of the growing season. The $r_s$ values ranged from a minimum of 22.4 s m$^{-1}$ to a maximum of 149 s m$^{-1}$ with a seasonal average of 63 s m$^{-1}$. The seasonal minimum $r_s$ (22.4 s m$^{-1}$) was measured on July 26 at 4:00 p.m. The microclimatic conditions at that time were characteristic of high atmospheric evaporative demand; $R_n$ was 577 W m$^{-2}$, air temperature was extremely high as 31.6°C, wind speed was 3.4 m s$^{-1}$, and VPD was 1.8 kPa. The seasonal maximum $r_s$ value (149 s m$^{-1}$) was measured on September 12 at 12:00 p.m. This was during the late growing season, and the high $r_s$ is most likely due to leaf aging and senescence. On September 12, the microclimatic conditions were $R_n$ = 429 W m$^{-2}$, air temperature = 23.5°C, wind speed = 5.1 m s$^{-1}$, and VPD = 1.0 kPa. The spike in $r_s$ on July 20 at 9:00 a.m. (fig. 2) was due to cloudy conditions and the typical coolness and low VPD (0.34 kPa) of morning hours. The highest $r_s$ value of 149 s m$^{-1}$ that was measured in this research, potentially lower than the values reported in the literature for soybean, was due to a combination of several factors, such as the well-watered conditions of soybean under subsurface drip irrigation, lower than long-term average air temperatures in June and July, considerably greater than long-term average relative humidity throughout the growing season, greater rainfall amounts during the peak atmospheric demand periods in July and August, the physiological differences between the soybean variety grown in this study and those studied in the literature, differences in performance between the instruments used to measure $r_s$, and combination of all these factors.

Soybean LAI (fig. 2) was 1.1 in late June, peaked at 5.1 in August, and the end-season value in late September was 1.9, with a seasonal average of 3.9 (from June 22 to September 20). As LAI increased to the maximum during the mid-growing season, $r_s$ decreased to its lowest seasonal values. After late August, due to senescence and increased $r_s$ of aged leaves, $r_s$ increased rapidly as LAI also sharply decreased. Monteith et al. (1965) observed a similar seasonal trend in $r_s$ in the late growing season and related it to increased epidermal resistance as leaves aged. Slatyer and Bierhuizen (1964) and Brown and Pratt (1965) discussed the increase in $r_s$ toward the end of the season and observed that the stomata of older leaves became less responsive and remained only partly open, even at midday with sufficient sunshine.

### Transferability of J-Model and NMJ-Model from Maize to Soybean

In this section, the transferability of the J-model and the NMJ-model developed for maize to estimate $r_s$ for soybean is evaluated. In Irmak and Mutiibwa (2009), the two models were calibrated for maize, and the models produced very good results, estimating field-measured $r_s$ with r$^2$ =

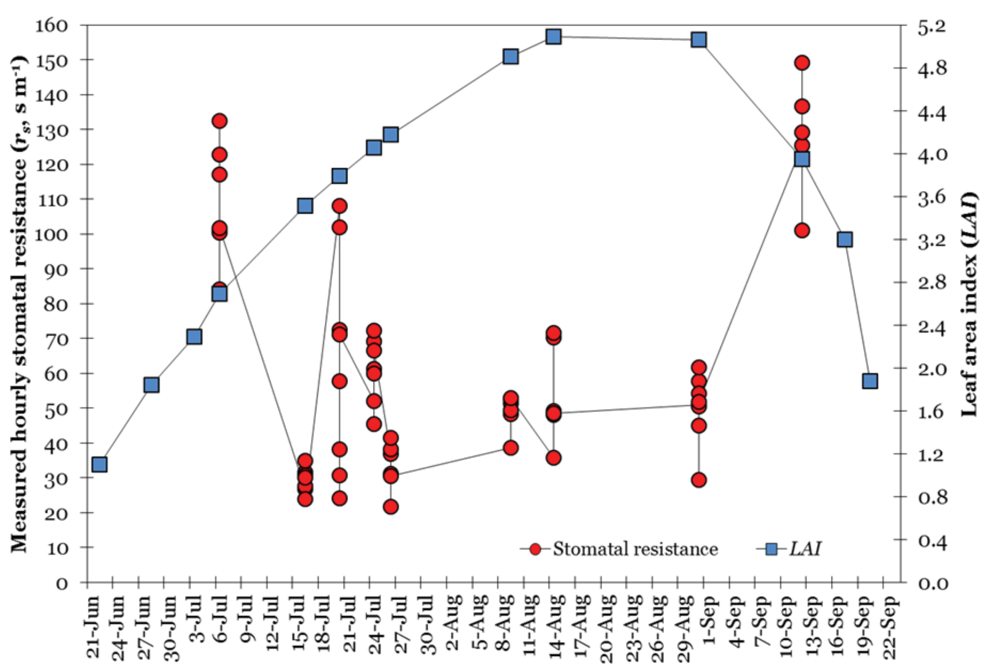


**Figure 2. Seasonal pattern of measured hourly stomatal resistance ($r_s$) and green LAI for soybean during the 2007 growing season.**

0.74, RMSD = 48.8 s m$^{-1}$ for the J-model, and $r^2$ = 0.74, RMSD = 50.1 s m$^{-1}$ for the NMJ-model. In this study, first without recalibration, the maize-calibrated models were used to estimate $r_s$ for soybean in a different year. Figures 3a and 3b show scatter plots of the J-model and NMJ-model estimates against measured $r_s$. Figure 3a shows that the maize-calibrated J-model substantially overestimated $r_s$ for soybean. The model $r^2$ was 0.38 and RMSD was 94.4 s m$^{-1}$, a significant deviation in the model's performance for soybean relative to its performance for maize. Before calibration, the NMJ-model overestimated measured soybean $r_s$ with a low $r^2$ of 0.30 and a very high RMSD of 166 s m$^{-1}$, a significant lapse in the performance of the model for soybean relative to maize. These results indicate the inherent limitation of J-type models that are calibrated for maize in estimating $r_s$ for soybean due to differences in the two crops' basic physiologic functions and their different photosynthetic pathways, which are implicitly imbedded in the model coefficients during calibration. These results also indicate that re-parameterization of J-type models results in crop-specific parameter (variable) coefficients, limiting their transferability to other crops and/or different environments. These models are empirical representations of the behavior of a very complex biological system, rather than representtations of simple physics of the system. Nevertheless, the models are applicable and valuable within their limits of validity (Raupach and Finnigan, 1988).

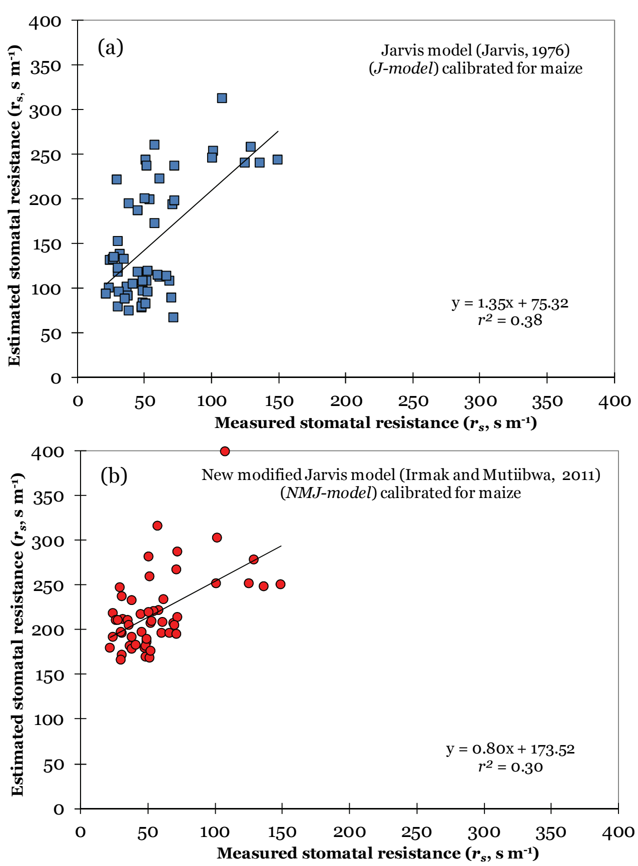


**Figure 3. Relationship between maize-calibrated stomatal resistance ($r_s$) models used to estimate soybean $r_s$: (a) Jarvis (1976) model (J-model), and (b) new modified Jarvis model (NMJ-model).**

Jarvis (1976) studied mainly forest canopies [Douglas fir (*Pseudotsuga menziesii*), Sitka spruce (*Picea sitchensis*), and Scots pine (*Pinus sylvestris*)] to develop his original model to estimate stomatal conductance. Our results demonstrate the need for re-parameterization of J-type models for accurate estimation of $r_s$ of a specific crop. The physiological structure differences between maize and soybean are primary reasons for the non-transferability of the maize model to soybean (Kirkham, 2005). The physiological differences between maize and soybean result in two different photosynthetic systems, and this results in their having two different stomatal resistances under the same conditions. Maize is a C4 plant and soybean is a C3 plant, and their stomata are anatomically different. C4 plants have dumbbell-shaped stomata, whereas C3 plants have bean-shaped stomata that function differently under the same environmental conditions. In general, the stomata of C4 plants have higher stomatal resistance than those of C3 plants. Differences in the shape, size, and distribution and changes in the growth of stomata with the development of the plant also contribute to the differences in stomatal response between maize and soybean (Kirkham, 2005, pp. 382-382) to the same environmental conditions. Kirkham (2011, pp. 172-174) provides an excellent and in-depth comparisons of the differences in stomatal functions between C4 and C3 plants.

### Calibration and Validation of Stomatal Resistance Models for Soybean

After assessing the performance of the maize-calibrated J-model and NMJ-model for estimating $r_s$ for soybean (with poor performance), the models were re-calibrated and re-parameterized for soybean by parameter optimization. The results are presented in table 3 and figures 4a and 4b for calibration and in figures 5a and 5b for validation. Compared to the maize-optimized parameters of the J-model, as presented by Irmak and Mutiibwa (2009), some of the soybean-optimized parameters were very similar (i.e., $b_2$ and $b_3$ coefficients), and others were substantially different (i.e., $b_1$, $b_4$, and $b_5$ coefficients). The optimization of the J-model (fig. 4a) resulted in a good $r^2$ of 0.63 and a small RMSD of 13.3 s m$^{-1}$ (table 3). The model underestimated $r_s$ by less than 30% and had a modeling efficiency (EF) of 0.22 (table 3). Overall, the calibration of the J-model yielded moderate results. However, for the validation (fig. 5a), the model performance was poor. The model substantially underestimated $r_s$ and was seemingly insensitive to changes in measured soybean $r_s$ with $r^2$ = 0.09, RMSD = 43.5 s m$^{-1}$, and EF = 0.78. Although the model $r^2$ is low, the good EF and RMSD statistics indicate that the J-model was still able to estimate the trends in soybean $r_s$, but not the magnitudes. When Jarvis (1976) presented the original model, his results showed that the model accounted for 51% and 73% of the variation in $r_s$ of two different datasets, and some of the variations in performance results in his study were attributed to inadequacies in the distribution of the data rather than to inadequacies in the model. Stomatal resistance is an extremely intermittent process, variant on leaf, plant, and field-level conditions. Thus, characterizing a single average

Table 3. Optimized values of parameters used in equations 2, 3, 4, and 6 to estimate soybean stomatal resistance ($r_s$) using the Jarvis (1976) model (J-model) and the new modified Jarvis (1976) model (NMJ-model): RMSD = root mean square difference between measured and estimated $r_s$, and EF = modeling efficiency.

| Model and Parameters after Optimization | Calibration RMSD ($s\ m^{-1}$) | Calibration $r^2$ | Calibration EF | Validation RMSD ($s\ m^{-1}$) | Validation $r^2$ | Validation EF |
|---|---|---|---|---|---|---|
| J-model | 13.3 | 0.63 | 0.22 | 43.5 | 0.09 | 0.78 |
| $b_1 = 3.7933$ | | | | | | |
| $b_2 = 1.88 \times 10^{-5}$ | | | | | | |
| $b_3 = 0.036$ | | | | | | |
| $b_4 = 0.1061$ | | | | | | |
| $b_5 = 0.00325$ | | | | | | |
| $b_6 = 1.320$ | | | | | | |
| NMJ-model | 13.7 | 0.71 | 0.59 | 38.4 | 0.83 | 0.75 |
| $a_0 = 3010$ | | | | | | |
| $a_1 = 0.514$ | | | | | | |
| $a_2 = 0.000268$ | | | | | | |
| $a_3 = 613.4$ | | | | | | |
| $a_4 = 0.036$ | | | | | | |
| $a_5 = 0.014$ | | | | | | |

value over a field for a given hour is a simple and useful concept; however, the depiction is a coarse assumption.

The NMJ-model calibration results for soybean are presented in figure 4b and table 3. Compared to the maize-optimized parameters of the NMJ-model presented by Irmak and Mutiibwa (2009), the soybean-optimized parameters $a_2$, $a_3$, and $a_5$ are substantially different. The NMJ-model calibrated better than the J-model, resulting in a higher $r^2$ of 0.71, a smaller RMSD of 13.7 $s\ m^{-1}$, and EF of 0.59. Given that the lowest measured $r_s$ was 22.4 $s\ m^{-1}$, an RMSD of 13.7 $s\ m^{-1}$ was an indication of a small calibration error, but is also an indication that the model's predictive ability was within acceptable limits. The model was able to account for 71% of the variation in measured $r_s$ of soybean. The calibrated model slightly underestimated measured $r_s$ with a slope of 0.99 (fig. 4b).

In general, model validation helps to establish a confidence in the calibration. A model is considered to be verified if its accuracy and predictive capability have been proven to be within acceptable limits of error by testing the independency of the calibration data (Konikow, 1978). The NMJ-model validation on an independent dataset produced superior results of $r^2 = 0.83$, RMSD = 38.4 $s\ m^{-1}$, and EF = 0.75. The model was able to explain more than 80% of the variation in the measured soybean $r_s$. This is a robust performance for the model, even slightly better than the model performance over maize canopy ($r^2 = 0.74$, RMSD = 50.1 $s\ m^{-1}$) observed by Irmak and Mutiibwa (2009). The RMSD of 38.4 $s\ m^{-1}$ is within the acceptable limits of error when the ranges of measured $r_s$ for soybean canopy are considered (fig. 2), as well as the extremely difficult nature

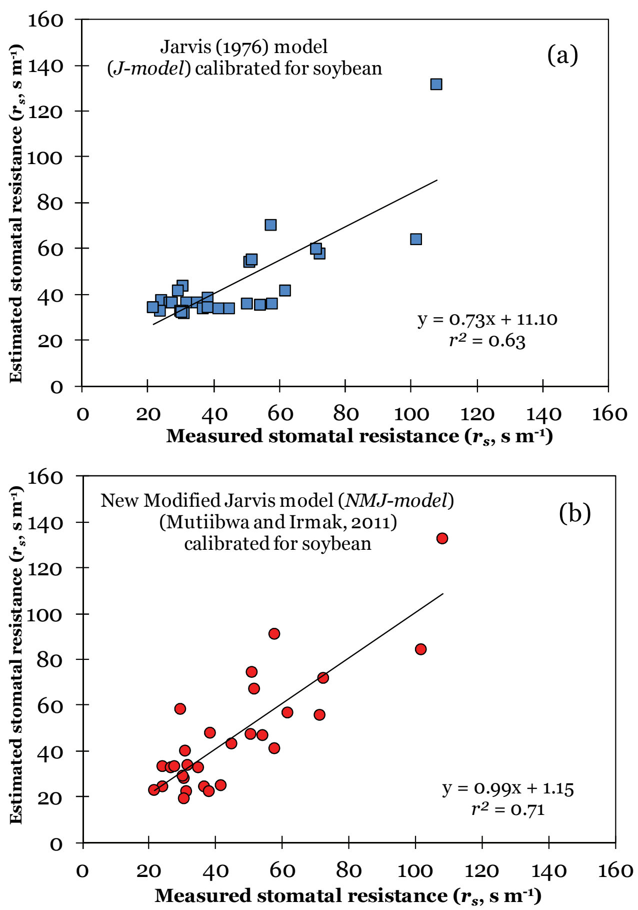


Figure 4. Relationship between measured vs. estimated stomatal resistance ($r_s$) for soybean canopy during calibration: (a) Jarvis (1976) model (J-model), and (b) new modified Jarvis model (NMJ-model).

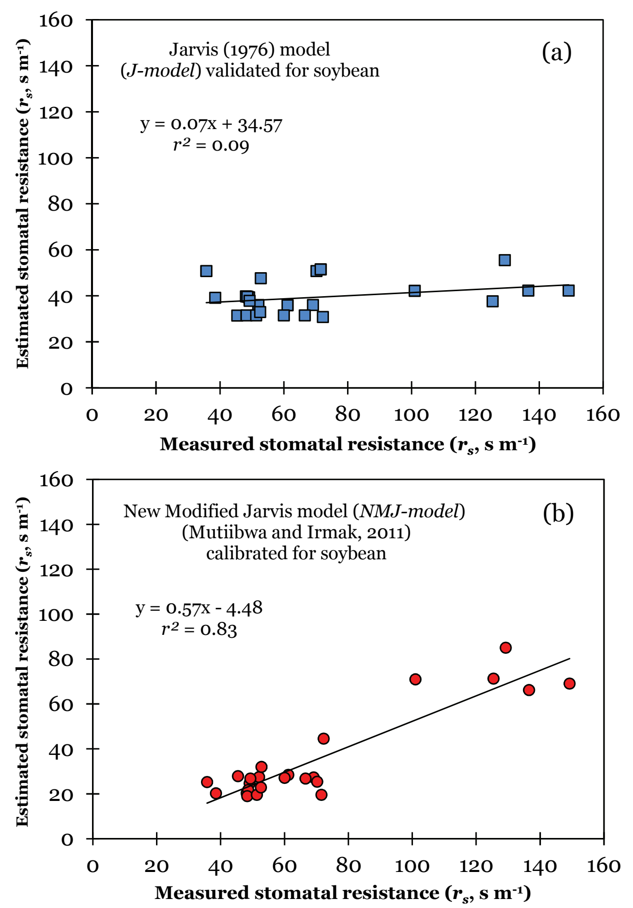


Figure 5. Relationship between measured vs. estimated stomatal resistance ($r_s$) for soybean canopy using models re-parameterized for soybean during validation: (a) Jarvis (1976) model (J-model), and (b) new modified Jarvis model (NMJ-model).

of modeling $r_s$ with great accuracy, especially on a short (hourly) time step. The EF being close to 1 is an indication of the model's ability to explain the variance of the measured $r_s$. The EF value of 0.75 for the soybean crop and 0.73 for the maize crop (Irmak and Mutiibwa, 2009) and similarities in the $r^2$ and RMSD values demonstrate the consistency of the model's good performance in estimating $r_s$ for different canopies if well calibrated for a specific crop.

Similar to other Jarvis-type models, the NMJ-model performance can be further improved with integration of the complex interaction effect of the variables. Nonetheless, using the multiple regression procedure on the primary independent variables that drive $r_s$, our validation results, as well as those observed by Irmak and Mutiibwa (2009), demonstrate the practical accuracy of estimating $r_s$ using the NMJ-model for soybean and maize crops, with crop-specific calibration parameters, and that NMJ-model can be extended to other crops by field measurements of $r_s$ and re-calibration/re-parameterization of the model parameters. The enhanced modeling of $r_s$ by the NMJ-model is attributed to the integration of the effect of LAI variation into the model. As such, the model accounts for the effect of plant development on $r_s$ during the growing season. The impact of the added LAI and $r_{s\_min}$ term [$r_{s_min}$exp(-LAI)] was assessed in figure 8 of Irmak and Mutiibwa (2009). Their results showed that most of the contribution of the LAI term to the modeling of $r_s$ occurred during the partial canopy phase (LAI < 3) of the growing season and late in the season during the leaf aging and leaf senescence stage.

### Sensitivity Analysis of NMJ-Model

Owing to the uncertainties in the calibration procedure, the parameter values used in the calibrated model may not be very precise. Consequently, the calibrated parameters may not accurately represent the biological system under a different set of conditions or environmental stresses (Anderson and Woessner, 1992). Therefore, the primary purpose of sensitivity analysis in this study is to evaluate the uncertainties in the calibrated parameters of the NMJ-model and quantify the plausible relative error introduced in the estimated soybean $r_s$. Figures 6a through 6g show the effect of changes in the calibrated parameters of the NMJ-model on the $r_s$ estimates. The parameters in the subfunctions of each climatic variable and the climatic variables themselves (because they are independent) were varied to quantify the respective relative error in $r_s$. Therefore, the response function of $r_s$ due to changes in the parameters of a given subfunction of a climatic variable is likely to be similar to changes in that climatic variable.

The sensitivity and elasticity analyses results on parameters $a_0$ and $a_1$ of the PPFD subfunction in the NMJ-model are presented in figures 6a and 6b. Parameter $a_0$ (fig. 6a), which was calibrated at a value of 3010 s $m^{-1}$ (table 3), was systematically varied from 30.11 (-99%) to 6000 (100%). Figure 6a shows that the relative change (%) in $r_s$ was very sensitive to relative changes (%) to $a_0$ between 30.11 (-99%) and 4515 (50%). For greater than 50% change in $a_0$, $r_s$ estimates became relatively insensitive. The elasticity function is constant between 30.11 (-99%) and 4515 (50%) change in parameter $a_0$, an indication that the sensitivity of $r_s$ to $a_0$ in this range is a linear function. The threshold is at about 4515 (50%), beyond which the sensitivity of $r_s$ to changes in parameter $a_0$ diminishes. This could be the point at which PPFD becomes non-limiting in driving $r_s$ with the stomata fully open. These results indicate that any uncertainties introducing errors between 30.11 (-99%) and 4515 (50%) will linearly, and probably significantly, affect the $r_s$ estimates using the NMJ-model. The relative error induced in $r_s$ is between -96.7% and 48.9%. Therefore for accurate estimates of $r_s$, uncertainties in parameter $a_0$ should not exceed -5% and 5%, in which case the relative error in $r_s$ will be within 4.5%.

The sensitivity and elasticity of analysis of $r_s$ with respect to parameter $a_1$ are presented in figure 6b. Parameter $a_1$, which was calibrated at a value of -0.514, was varied from -0.508 (-99%) to -1.027 (100%). Among all parameters, $r_s$ was most sensitive to relative changes in parameter $a_1$, especially between 0.005135 (-99%) and 0.488 (-10%). This could be attributed to the exponential nature of the parameter in the NMJ-model (eq. 6). The $r_s$ estimate was still, but moderately less, sensitive to changes in $a_1$ above -10%. Similar to parameter $a_0$, this could be due to PPFD becoming non-limiting, with the stomata already fully open. The elasticities show that the sensitivity function of $r_s$ to $a_1$ is an exponential decay function. From the elasticity function, it also appears that $r_s$ becomes asymptotically insensitive to changes in $a_1$ beyond 0.488 (-10%). In other words, $r_s$ is very elastic between 0.005135 (-9%) and 0.488 (-10%), beyond which point the response becomes inelastic. Due to this apparent high and non-linear sensitivity of $r_s$ to $a_1$, the parameter uncertainty should not exceed the range of -0.508 (-1%) and -0.519 (1%), such that the error in estimated $r_s$ is kept between -3.5% and 3.6%. This sensitivity and elasticity analysis of the PPFD subfunction depicts the plausible extent of errors introduced in modeling $r_s$ due to plausible uncertainties in parameters $a_0$ and $a_1$. One of the sources of uncertainties in the parameters of the PPFD subfunction may be the characteristic of hysteresis observed in $r_s$ and light functions. Other potential sources of uncertainties include measurement errors and field data inadequacy to fit the PPFD-$r_s$ response subfunction.

Because of the continuous effect of VPD, along with PPFD, on $r_s$, these variables are considered the primary stomatal control factors for most crops (Kaufmann, 1982). The sensitivity and elasticity analysis of parameters $a_2$ and $a_3$ in the VPD subfunction of the NMJ-model are presented in figures 6c and 6d. Parameter $a_2$, which was calibrated at a value of 0.036, was systematically varied from 0.00036 (-99%) to 0.072 (100%), and the resulting relative error in $r_s$ ranged from 0.046% to -0.048%, respectively. Parameter $a_3$ (fig. 6d), which was calibrated at a value of 0.0141, was systematically varied from 0.000141 (-99%) to 0.0283 (100%), and the resulting relative error in $r_s$ ranged from 0.0461% to -0.0458%, respectively. Figures 6c and 6d show that the relative change in $r_s$ due to the relative change in parameters $a_2$

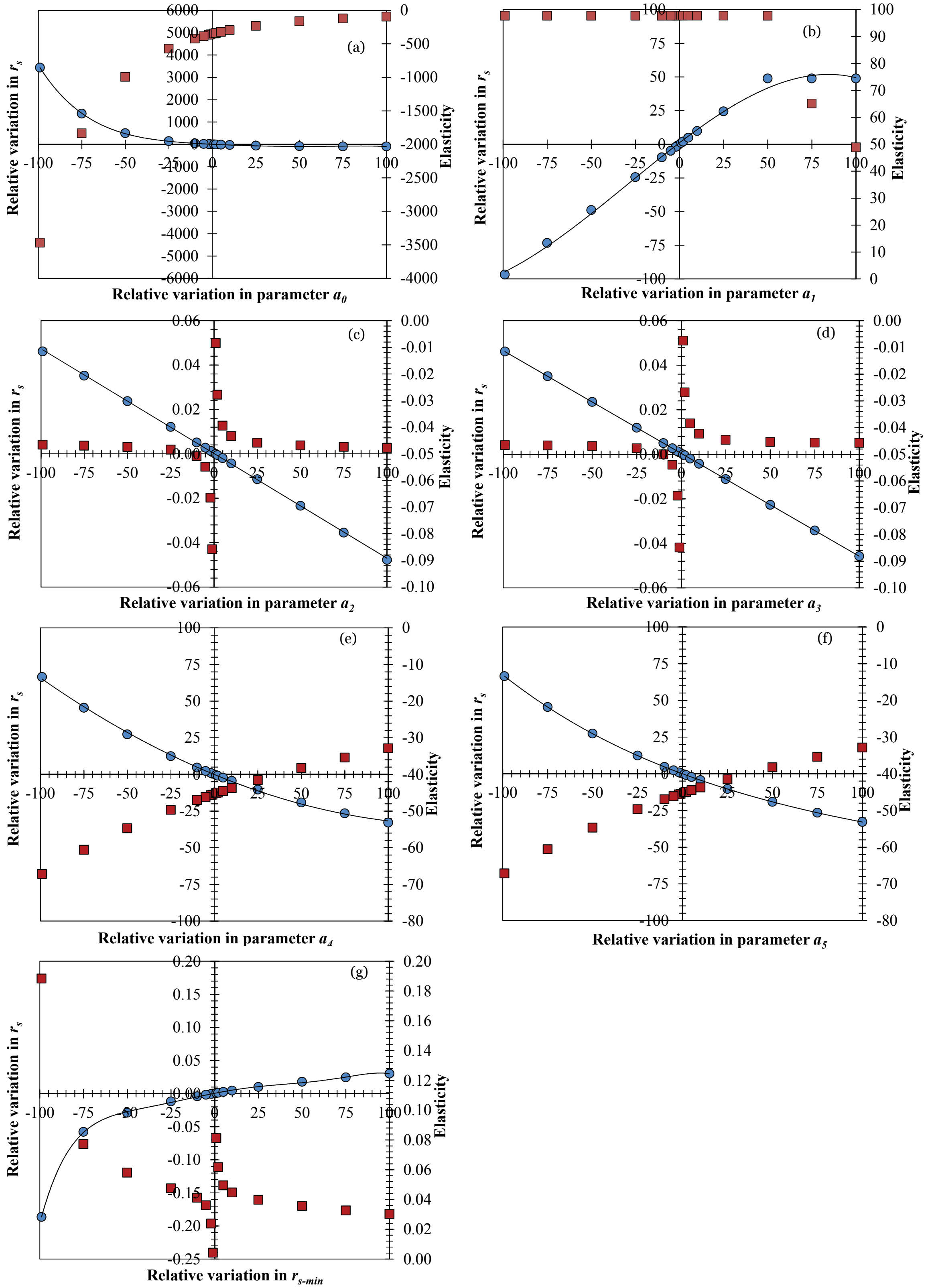

**Figure 6. NMJ-model output of $r_s$ sensitivity to the parameters of (a and b) photosynthetic photon flux density (PPFD) subfunction, (c and d) vapor pressure deficit (VPD) subfunction, (e and f) air temperature ($T_a$) subfunction, and (g) minimum stomatal resistance ($r_{s\_min}$) subfunction. Squares represent elasticity, and circles represent relative variation in $r_s$.**

and $a_3$ is a linear function. The linear relationships of both parameters have a percentage slope of -0.05, which is equivalent to the constant value of the elasticity function shown in the figures. Thorpe et al. (1980) and Monteith (1965) also observed a linear relationship between $r_s$ and VPD from field measurements. As mentioned earlier, varying the parameters in a subfunction effectively varies the microclimatic variable independently, in this case VPD, thus producing a similar response function of $r_s$ to the changes in the microclimatic variable. The elasticity values reported in figures 6c and 6d are negative and less than -1, which means that increases in parameters $a_2$ and $a_3$ result in a relatively small decrease in $r_s$. Normally, if soil water content is not limiting, which was the case in this experiment, then $r_s$ responds by decreasing (stomatal opening as the resistance to water vapor flow decreases) as VPD increases. The sensitivity and elasticity of $r_s$ in response to changes in VPD subfunction parameters is not as drastic as that of PPFD; this could be due to generally gradual changes in relative humidity in the natural environment. In contrast, PPFD is usually intermittent due to atmospheric and cloudiness variations, in addition to the distribution variability of PPFD in the canopy, especially during the windy conditions. The elasticity function is a constant function at -0.05, apart from between -10% and 10% of relative change in parameters $a_2$ and $a_3$. Within this range (-10% and 10%), the function asymptotically approaches the nominal value (0%) from both sides of the plot, as shown in figures 6c and 6d. In general, due to the low sensitivity of $r_s$ to relative changes in parameters $a_2$ and $a_3$, uncertainties in these parameters within -25% to 25% may be acceptable, with marginal impact of about -0.011% to 0.012% on $r_s$ estimates.

The effect of air temperature on $r_s$ is considered secondary (Kaufmann, 1982) because its effect is limited during extreme conditions. In addition, due to the strong correlation between temperature and VPD, the effect of temperature on $r_s$ is implicitly imbedded in VPD, and it is difficult to determine its impact on $r_s$ independently. The sensitivity and elasticity analysis of parameters $a_4$ and $a_5$ in the temperature subfunction are presented in figures 6e and 6f. Parameter $a_4$, which was calibrated at a value of 0.000268, was systematically varied from 0.00000268 (-99%) to 0.000535 (100%), and the resulting relative change in $r_s$ ranged from 66.5% to -32.9%, respectively. Parameter $a_5$, which was calibrated at a value of 613.356, was systematically varied from 6.134 (-99%) to 1226.712 (100%), and the resulting relative change in $r_s$ ranged from 66.5% to -32.9%, respectively. Due to the magnitude of the relative change in $r_s$ estimates, it appears that $r_s$ is more sensitive to changes in parameters $a_4$ and $a_5$ than parameters $a_2$ and $a_3$ of the VPD subfunction. The elasticities show a negative nonlinear relationship greater than -1. This means that $r_s$ estimates are highly sensitive and dynamic to uncertainties in the parameters of the temperature subfunction, as compared with the VPD subfunction. An uncertainty of 1% change in parameters $a_4$ and $a_5$ resulted in a relative change of about 0.05% in $r_s$. However, beyond 10% change in parameters $a_4$ and $a_5$, the change in $r_s$ was 5% or more. With this observation, the uncertainty in parameters $a_4$ and $a_5$ should range within -10% and 10%. With this range of uncertainty in the parameters, the errors in $r_s$ are kept within 4.7% and -4.4%. Therefore, the calibration of temperature subfunction parameters should be determined with greater precision than the VPD subfunction parameters.

The sensitivity of estimated $r_s$ to relative changes in $r_{s\_min}$ is presented in figure 6g. The $r_{s\_min}$ was a field-measured value of 22.4 s m$^{-1}$ in this experiment and was systematically varied from 0.224 (-99%) to 44.8 (100%), and the resulting relative change in $r_s$ ranged from -0.1864% to 0.0302%, respectively. The sensitive function of relative changes in $r_s$ due to uncertainties in $r_{s\_min}$ is non-linear. Figure 6g shows that estimates of $r_s$ are more sensitive to relative changes in $r_{s\_min}$ below -50%. However, above -50%, the function tapers off and becomes almost linear as $r_s$ becomes relatively insensitive to changes in $r_{s\_min}$. Between -50% and 100% relative change in $r_{s\_min}$, the rate of change in $r_s$ (or % slope) is 0.03. Given the small errors introduced in estimated $r_s$ over a wide range of uncertainties in $r_{s\_min}$, estimated $r_s$ appears to be generally insensitive to $r_{s\_min}$. The elasticities are positive and less than 1, which is a further indication that $r_s$ is inelastic to changes in $r_{s\_min}$. This is an important observation because the $r_{s\_min}$ of any given crop is an extremely difficult value to determine in the field, which requires $r_s$ measurements under a variety of weather conditions and growth stages during the entire growing season. Obtaining the $r_{s\_min}$ of a crop requires having many ideal conditions in place, including optimal atmospheric evaporative demand, optimal soil water content, and a healthy crop at an optimal development stage. Kelliher et al. (1995) described the optimal environmental conditions required to achieve $r_{s\_min}$ for a vegetation surface as plentiful of soil water, adequate light, low humidity deficit, and optimal temperature. As mentioned earlier, in this experiment, the $r_{s\_min}$ (22.4 s m$^{-1}$) was the lowest measured soybean $r_s$ from the field measurements over the entire growing season. Although the results show that the NMJ-model is not significantly impacted by uncertainties in $r_{s\_min}$, effort should be taken to determine a precise $r_{s\_min}$ to avoid cumulative uncertainties from the other calibrated parameters in the model, as discussed above.

## SUMMARY AND CONCLUSIONS

This progression study of the new modified Jarvis model (NMJ-model), developed for maize by Irmak and Mutiibwa (2009), extends the model to soybean and presents an analysis of model performance, calibration, validation, sensitivity, and elasticity of leaf stomatal resistance ($r_s$) estimates to uncertainties in the calibrated model parameters. The study evaluated the transferability of the original Jarvis (1976) model (J-model) and the new modified Jarvis model (NMJ-model) that were calibrated/parameterized for maize to estimate $r_s$ for soybean. The original maize-calibrated NMJ-model and J-model were not able to estimate soybean $r_s$ with a reasonable accuracy. The inherent limitation in the transferability of Jarvis-type models that are calibrated/re-parameterized for a specific crop to another crop is due to the differences in the crops' phenomenological development and physiological functions and differences in the response of $r_s$ to the same environmental variables between different crops. These differences justify the need for re-parameterization of models for specific crops for more accurate and robust $r_s$ estimates. The J-model and NMJ-model were re-calibrated by parameter optimization for soybean. The J-model calibrated well for soybean. However, the validation had mixed results. The model underestimated $r_s$, but had good modeling efficiency (EF = 0.78) and relatively low root mean square difference (RMSD = 43.5 s $m^{-1}$) between the measured and estimated soybean $r_s$. The NMJ-model calibrated better than the J-model, resulting in a good $r^2$ (0.71) and a small RMSD (13.7 s $m^{-1}$), slightly underestimating the measured $r_s$ with a slope of 0.99. The NMJ-model validation on an independent dataset produced superior results. The NMJ-model was able to explain more than 80% of the variation in the measured $r_s$, with an RMSD of 38.4 s $m^{-1}$ and EF of 0.75. The results were slightly better than the performance of the model observed over non-stressed maize canopy by Irmak and Mutiibwa (2009).

These results show the robustness and practical accuracy of the NMJ-model in estimating $r_s$ over different canopies, if the model is well calibrated or re-parameterized for a specific crop. The enhanced modeling of $r_s$ by the NMJ-model was, in part, attributed to the integration of the term $A^{\exp(1/LAI)}$ to account for the effect of LAI on $r_s$, especially during partial canopy (early season) and leaf aging and/or senescence (late season). Overall, the results of this study and the observations by Irmak and Mutiibwa (2009) confirmed that the NMJ-model can provide robust and accurate $r_s$ estimates for maize and soybean canopies and that it can be extended to other crops by field measurements of $r_s$ and re-calibration/re-parameterization of the model parameters.

Detailed sensitivity and elasticity analyses were conducted to quantify the potential relative error introduced in $r_s$ estimates due to plausible uncertainties in the NMJ-model parameters (eq. 6). The sensitivity and elasticity analysis of parameter $a_0$ of the PPFD subfunction showed that the $r_s$ was very sensitive to relative change in $a_0$ between -99% and 50%. For higher than 50% relative change in $a_0$, $r_s$ became relatively insensitive. The elasticity function was constant between -99% and 50% relative changes in parameter $a_0$, an indication that the sensitivity of $r_s$ to $a_0$ in this range is linear. The threshold for the parameter was at about 4515 (50%), beyond which $r_s$ sensitivity to changes in parameter $a_0$ diminished. For accurate estimates of $r_s$, uncertainties in parameter $a_0$ should not exceed -5% and 5% to ensure that the relative error in $r_s$ is within -4.5% and 4.5%. Among all parameters, $r_s$ estimates were most sensitive to uncertainties introduced in parameter $a_1$ of the PPFD subfunction. For accurate estimates of $r_s$, uncertainties in parameter $a_1$ should not exceed the range of -2% and 2%, so that the error in estimated $r_s$ is kept between -3.5% and 3.6%. The sensitivity and elasticity of $r_s$ in response to changes in the VPD subfunction parameters were not as high as for the PPFD subfunction parameters. Therefore, uncertainties in parameters $a_2$ and $a_3$ between -25% and 25% may be acceptable, with marginal impact of -0.011% to 0.012% on $r_s$ estimates. The uncertainties in temperature subfunction parameters $a_4$ and $a_5$ had a non-linear relationship with relative change in estimated $r_s$. The uncertainty in parameters $a_4$ and $a_5$ should range within -10% and 10%, and the calibration of these parameters should be determined with greater precision as compared with the VPD subfunction parameters. The sensitive function of $r_s$ relative changes due to uncertainties in $r_{s\_min}$ was both non-linear and linear in two sections. In the linear section, $r_s$ was relatively insensitive to uncertainties in $r_{s\_min}$. In general, small errors were introduced in estimated $r_s$ over a wide range of uncertainties in $r_{s\_min}$. This is an important observation because $r_{s\_min}$ is a difficult value to determine in field conditions. The uncertainties introduced with the aforementioned parameters into the NMJ-model can be controlled or reduced, to a degree, by substantially increasing the number of stomatal resistance measurements to account for the $r_s$ response to a given variable under a wide range of conditions in the model calibration/re-parameterization process.

## References


Anderson, M. P., and W. W. Woessner. 1992. *Applied Groundwater Modeling*. New York, N.Y.: Academic Press.

Ball, J. T., I. E. Woodrow, and I. A. Berry. 1987. A model predicting stomatal conductance and its contribution to the control of photosynthesis under different environmental conditions. In *Progress in Photosynthesis Research*, 4: 221-224. J. Biggins, ed. Dordrecht, The Netherlands.

Brown, W. V., and G. A. Pratt. 1965. Stomatal inactivity in grasses. *Southwest Naturalist* 10(1): 48-56.

Farquhar, G. D. 1978. Feedforward responses of stomata to humidity. *Australian J. Plant Physiol*. 5(6): 787-800.

Farquhar, G. D., S. von Caemmerer, and J. A. Berry. 1980. A biochemical model of photosynthetic $CO_2$ assimilation in leaves of C3 species. *Planta* 149(1): 78-90.

Finnigan, J. J., and M. R. Raupach. 1987. Modern theory of transfer in plant canopies in relation to stomatal characteristics. In *Stomatal Physiology*, 385-429. E. Zeiger, G. D. Farquhar, and I. R. Cowan, eds. Palo Alto, Cal.: Stanford University Press.

Green, S. R., and K. G. McNaughton. 1997. Modeling effective stomatal resistance for calculating transpiration from an apple tree. *Agric. Forest Meteorol*. 83(1-2): 1-26.

Hamby, D. M. 1994. A review of techniques for parameter sensitivity analysis of environmental models. *Environ. Monit. and Assess.* 32(2): 135-154.

Irmak, S. 2010. Nebraska Water and Energy Flux Measurement, Modeling, and Research Network (NEBFLUX). *Trans. ASABE* 53(4): 1097-1115.

Irmak, S., and D. Mutiibwa. 2009. On the dynamics of stomatal resistance: Relationships between stomatal behavior and micrometeorological variables and performance of Jarvis-type parameterization. *Trans. ASABE* 52(6): 1923-1939.

Irmak, S., and D. Mutiibwa. 2010. On the dynamics of canopy resistance: Generalized-linear estimation and its relationships with primary micrometeorological variables. *Water Resources Res.* 46(8): W08526, doi: 10.1029/2009WR008484.

Jarvis, P. G. 1976. The interpretation of the variations in leaf water potential and stomatal conductance found in canopies in the field. *Phil. Trans. Royal Soc. London B* 273(927): 593-610.

Jarvis, P. G., and K. G. McNaughton. 1986. Stomatal control of transpiration: Scaling up from leaf to region. *Adv. in Ecol. Res*. 15(1): 1-49.

Kaufmann, R. M. 1982. Evaluation of season, temperature, and water stress effects on stomata using a leaf conductance model. *Plant Physiol*. 69(5): 1023-1026.

Kelliher, F. M., R. Leuning, M. R. Raupach, and E. D. Schulze. 1995. Maximum conductance for evaporation from global vegetation types. *Agric. Forest Meteorol*. 73(1-2): 1-16.
Kirkham, M. B. 2005. *Principles of Soil and Plant Water Relations*. Amsterdam, the Netherlands: Elsevier Academic.
Kirkham, M. B. 2011. *Elevated Carbon Dioxide: Impacts on Soil and Water Relations*. Boca Raton, Fla.: CRC Press.
Konikow, L. F. 1978. Calibration of groundwater models. In *Verification of Mathematical and Physical Models in Hydraulic Engineering*, 87-93. New York, N.Y.: ASCE.
Lohammar, T., S. Larsson, S. Linder, and O. Falk. 1980. FAST-simulation models of gaseous exchange in Scots pine. *Ecology Bulletin* (Stockholm) 32: 505-523.
Massman, W. J., and M. R. Kaufmann. 1991. Stomatal response to certain environmental factors: A comparison of models for subalpine trees in the Rocky Mountains. *Agric. Forest Meteorol*. 54(2-4): 155-167.
Monteith, J. L. 1965. Evaporation and the environment. In *Proc. XIXth Symp.: The State and Movement of Water in Living Organisms*, 19: 205-234. Cambridge, U.K.: Cambridge University Press.
Monteith, J. L., G. Szeicz, and P. E. Waggoner. 1965. The measurement and control of stomatal resistance in the field. *J. Appl. Ecol*. 2(2): 345-355.
Mutiibwa, D., and S. Irmak. 2011. On the scaling up soybean leaf level stomatal resistance to canopy resistance for one-step estimation of actual evapotranspiration. *Trans. ASABE* 54(1): 141-154.
Niyogi, D. S., and S. Raman. 1997. Comparison of four different stomatal resistance schemes using FIFE observations. *J. Appl. Meteorol*. 36(7): 903-917.
Noilhan, J., and S. Planton. 1989. A simple parameterization of land surface processes for meteorological models. *Mon. Weather Rev*. 117(3): 536-549.
Pleim, J., and A. Xiu. 1995. Development and testing of a surface flux and planetary boundary layer model for application in mesoscale models. *J. Appl. Meteorol*. 34(1): 16-32.
Raupach, M. R., and J. J. Finnigan. 1988. “Single-layer models of evaporation from plant canopies are incorrect but useful, whereas multilayer models are correct but useless”: Discuss. *Australian J. Plant Physiol*. 15(6): 705-716.
Slatyer, R. O., and J. F. Bierhuizen. 1964. Transpiration from cotton leaves under a range of environmental conditions in relation to internal and external diffusive resistances. *Australian J. Biol. Sci*. 17(1): 115-130.
Thomas, D. S., D. Eamus, and D. Bell. 1999. Optimization theory of stomatal behaviour: II. Stomatal responses of several tree species of north Australia to changes in light, soil and atmospheric water content, and temperature. *J. Exp. Botany* 50(332): 393-400.
Thompson, N., I. A. Barrie, and M. Ayles. 1981. The meteorological office rainfall and evaporation calculation system: MORECS. Hydrological Memorandum No. 45. Exeter, U.K.: Met Office.
Thorpe, M. R., B. Warrit, and J. J. Landsberg. 1980. Response of apple leaf stomata: A model for single leaves and a whole tree. *Plant Cell Environ*. 3(1): 23-27.
Viterbo, P., and A. Beljaars. 1995. An improved land-surface parameterization scheme in the ECMWF models and its validation. *J. Climate* 8(11): 2716-2748.